Possible Three-Dimensional Nematic Odd-Parity Superconductivity in Sr_2RuO_4

Wen Huang[1] and Hong Yao[1,2,3,*]
[1]Institute for Advanced Study, Tsinghua University, Beijing 100084, China
[2]State Key Laboratory of Low Dimensional Quantum Physics, Tsinghua University, Beijing 100084, China
[3]Collaborative Innovation Center of Quantum Matter, Beijing 100084, China

(Received 18 March 2018; published 12 October 2018)

The superconducting pairing in Sr_2RuO_4 is widely considered to be chiral p wave with $\vec{d}_{\boldsymbol{k}} \sim (k_x + ik_y)\hat{z}$, which belongs to the E_u representation of the crystalline D_{4h} group. However, this superconducting order appears hard to reconcile with a number of key experiments. In this Letter, based on symmetry analysis we discuss the possibility of odd-parity pairing with inherent three-dimensional character enforced by the interorbital interlayer coupling and the sizable spin-orbit coupling in the material. We focus on a yet unexplored E_u pairing, which contains finite $(k_z\hat{x}, k_z\hat{y})$ component in the gap function. Under appropriate circumstances a novel time-reversal invariant nematic pairing can be realized. This nematic superconducting state could make contact with some puzzling observations on Sr_2RuO_4, such as the absence of spontaneous edge current and no evidence of split transitions under uniaxial strains.

DOI: 10.1103/PhysRevLett.121.157002

Introduction.—Superconductivity in Sr_2RuO_4 was discovered [1] in 1994 and was immediately proposed to be of spin-triplet pairing in relation to the possible remnant ferromagnetic correlations in the material [2,3]. Over the years, multiple measurements show evidence of spin-triplet [4,5], odd-parity pairing [6], with the additional feature of time-reversal symmetry breaking (TRSB) [7,8]. These point to a possible chiral p-wave pairing [9–16] in the E_u representation, represented by the pairing function $\vec{d}_{\boldsymbol{k}} = (k_x \pm ik_y)\hat{z}$. Here "±" indicate the time-reversed pair of degenerate chiral states, and the direction of the $\vec{d}$ vector, $\hat{z}$ in this case, denotes the structure of Cooper pairing in spin space (see later). If confirmed, Sr_2RuO_4 will be a solid state analog of the well-known liquid ^{3}He A phase [17]. This state is topologically nontrivial, wherein the Cooper pairs carry nonvanishing quantized orbital angular momentum. It supports exotic excitations such as chiral edge states and Majorana zero modes in superconducting vortex cores. The latter is marked by non-Abelian braiding statistics crucial for topological quantum computation [18,19].

However, the chiral p-wave pairing still currently stands in conflict with a number of experimental observations. A prominent example is the absence of spontaneous edge current [20–22]. Existing measurements place an upper bound for the edge current over 3 orders of magnitude smaller than predicted for an isotropic single-band chiral p-wave model [23]. Other inconsistencies include but are not limited to abundant residual density of states going against the fully gapped nature of a chiral p wave [24,25], signatures reminiscent of the Pauli limiting behavior [26–29], and the absence of split transitions in the presence of external perturbations expected to lift the degeneracy of the two E_u components of the chiral order parameter, such as an in-plane magnetic field [29] and in-plane uniaxial strains [30,31], etc.

Recent years have seen a broad spectrum of theoretical attempts to resolve various aspects of the puzzle [32–68]. However, a consensus is still lacking regarding the exact pairing symmetry in Sr_2RuO_4. To this end, we take a different angle and study a possible alternative $\vec{d}$ vector in the E_u representation on account of the weak interorbital interlayer tunneling and the sizable spin-orbit coupling (SOC) [69–71] between the Ru $4d$ t_{2g}-orbitals—which introduce considerable three-dimensional spin-orbit entanglement as reported in photoemission studies [70]. In addition to the pairing in the channel $(k_x\hat{z}, k_y\hat{z})$, the $\vec{d}$ vector should contain a finite $(k_z\hat{x}, k_z\hat{y})$ pairing, thereby constituting a full 3D superconducting pairing. As we shall see, the interplay between these two pairing channels brings about an interesting possibility of a novel time-reversal invariant (TRI) nematic superconducting phase. Such a state is doubly degenerate, possesses symmetry-imposed point-nodal quasiparticle excitations (but could in principle support accidental nodal lines), and exhibits a broken rotational symmetry with respect to the underlying tetragonal crystal symmetry. In addition, in comparison with the chiral p-wave order, the nematic pairing could better explain the absence of split transitions under external perturbations that lift the degeneracy of the two E_u components, as we shall explain later.

In a similar vein, odd-parity nematic superconductivity has been proposed in the doped topological insulator, Bi_2Se_3 [72–74], which has strong SOC and whose resultant rotational symmetry breaking has been reported in a few measurements [75–79].

The Gingzburg-Landau theory.—The generic two-component odd-parity superconducting pairing function in the E_u representation reads

$$\hat{\Delta}_{\boldsymbol{k}} = i(\phi_1 \vec{d}_{1,\boldsymbol{k}}\cdot\vec{\sigma} + \phi_2 \vec{d}_{2,\boldsymbol{k}}\cdot\vec{\sigma})\sigma_y, \tag{1}$$

where $\phi_{1,2}$ label the order parameters associated with the two components, $\vec{d}_{i,\mathbf{k}}$ are real vectors denoting the spin structure of the two components of Cooper pairing. The components of $\vec{d}_{i,\boldsymbol{k}}$ contain appropriate form factors [e.g., Eq. (4)] which form a two-dimensional E_u representation of the underlying tetragonal crystalline space group D_{4h} [80,81]. Throughout the work we assume only intraband Cooper pairing near the Fermi level, as is appropriate for a weak-coupling superconductor.

In the absence of SOC, the $\vec{d}$ vectors can be written in a separable form, $\vec{d}_{i,\boldsymbol{k}} = \vec{d} f_{i,\boldsymbol{k}}$, due to full spin rotational invariance. Here, the form factors $f_{i,\boldsymbol{k}}$ act as the basis functions of the corresponding symmetry group. In the presence of SOC, Eq. (1) is more appropriately expressed in the pseudospin basis, whereby we would have duly accounted for the effects of SOC. In particular, since the spin and orbital degrees of freedom are now entangled, the $\vec{d}$ vector is locked with the momentum of the Bloch electron with pseudospin indices. In other words, the elements of the symmetry group operate simultaneously on the spin and the spatial coordinates.

We start our analyses with a phenomenological Gingzburg-Landau free energy. Up to the quartic order:

$$\begin{aligned} f = {} & r(T-T_c)(|\phi_1|^2 + |\phi_2|^2) + \beta(|\phi_1|^4 + |\phi_2|^4) \\ & + \beta_{12}|\phi_1|^2|\phi_2|^2 + \beta'(\phi_1^*\phi_2 + \phi_1\phi_2^*)^2. \end{aligned} \tag{2}$$

Within mean field, coefficients of the quartic terms determine the stable superconducting state. In Ref. [82] we derive the expressions for evaluating these coefficients, from where it is apparent that β and β_{12} are positive definite. By contrast, the sign of β' depends on the structure of $\vec{d}_{i,\boldsymbol{k}}$ and can be roughly approximated by

$$\beta' \approx C\langle(\vec{d}_{1,\boldsymbol{k}}\cdot\vec{d}_{2,\boldsymbol{k}})^2 - |\vec{d}_{1,\boldsymbol{k}}\times\vec{d}_{2,\boldsymbol{k}}|^2\rangle_{\mathrm{FS}}, \tag{3}$$

where C is a positive constant and $\langle\cdots\rangle_{\mathrm{FS}}$ denotes an integral over the Fermi surface. Similar expression was also obtained in Ref. [74]. By inspection, if $\beta' > 0$, ϕ_1 and ϕ_2 preferentially develop a $\pi/2$ phase difference, i.e., $\boldsymbol{\phi} = (\phi_1, \phi_2) = \phi(1, \pm i)$, thereby breaking time-reversal invariance, as for the chiral p-wave order; while if $\beta' < 0$, the system favors a TRI order parameter, $\boldsymbol{\phi} = \phi(1, \pm 1)$ or $\phi(1, 0)$. Note that the theory applies equally well to single- and multiband models.

Interlayer-coupling-enforced 3D $\vec{d}$ vector.—Thus far, the assignment of the possible $\vec{d}$ vector in Sr_2RuO_4 has been largely dictated by the considerations of its layered structure. In particular, the quasi-2D character of the electronic structure naturally leads one to conjecture the absence of interlayer Cooper pairing that takes the form of, e.g., $\Delta_{\boldsymbol{k}} \sim k_z$ in the p-wave channel. However, no particular symmetry constraint prohibits such a pairing. Indeed, interlayer pairings of one form or another have been considered in a few microscopic models formulated in different contexts [83–85].

TABLE I. Irreducible odd-parity representations of the D_{4h} group and the corresponding basis functions.

irrep.	basis function ($\vec{d}_{\boldsymbol{k}}$)
A_{1u}	$k_x\hat{x} + k_y\hat{y};\ k_z\hat{z}$
A_{2u}	$k_y\hat{x} - k_x\hat{y}$
B_{1u}	$k_x\hat{x} - k_y\hat{y}$
B_{2u}	$k_y\hat{x} + k_x\hat{y}$
E_u	$(k_x, k_y)\hat{z};\ (k_z\hat{x}, k_z\hat{y})$

According to the classification in Table I, when a k_z-like pairing does develop, the superconducting state in the E_u representation is more appropriately described by the following $\vec{d}$ vector,

$$\vec{d}_{1,\boldsymbol{k}} = k_x\hat{z} + \epsilon k_z\hat{x} \quad \text{and} \quad \vec{d}_{2,\boldsymbol{k}} = k_y\hat{z} + \epsilon k_z\hat{y}, \tag{4}$$

where ϵ is a nonuniversal real constant determined by the relative strength of the effective interactions responsible for the respective $(k_x, k_y)\hat{z}$ and $(k_z\hat{x}, k_z\hat{y})$ pairings, respectively. This alternative $\vec{d}$-vector texture was alluded to in Ref. [56].

Most previous quasi-two-dimensional spin-orbit coupled models of Sr_2RuO_4 do not support coexisting $(k_x, k_y)\hat{z}$ and $(k_z\hat{x}, k_z\hat{y})$ pairings. This is due to the absence of direct interorbital hopping (or hybridization) between the xy and the xz/yz orbitals in those models. To understand this, we study the corresponding single-particle Hamiltonian,

$$H = \sum_{\boldsymbol{k},s} \psi^\dagger_{\boldsymbol{k},s} \hat{H}_{0s}(\boldsymbol{k}) \psi_{\boldsymbol{k},s}, \tag{5}$$

where the sub-spinor $\psi_{\boldsymbol{k},s} = (c_{xz,\boldsymbol{k},s}, c_{yz,\boldsymbol{k},s}, c_{xy,\boldsymbol{k},-s})^T$ with $c_{a,\boldsymbol{k},s}$ annihilating a spin-s electron on the a orbital ($a = xz, yz, xy$), $s = \uparrow$ and $\downarrow$ denote up and down spins, and,

$$\hat{H}_{0s}(\boldsymbol{k}) = \begin{pmatrix} \xi_{xz,\boldsymbol{k}} & \lambda_{\boldsymbol{k}} - is\eta & i\eta \\ \lambda_{\boldsymbol{k}} + is\eta & \xi_{yz,\boldsymbol{k}} & -s\eta \\ -i\eta & -s\eta & \xi_{xy,\boldsymbol{k}} \end{pmatrix}, \tag{6}$$

with $\xi_{a,\boldsymbol{k}}$ given in Ref. [82]. Here $\lambda_{\boldsymbol{k}}$ is the interorbital hybridization between the quasi-1D xz and yz orbitals; and η is the strength of SOC. The eigenstates of Eq. (5) constitute the pseudospin electrons in the band representation. It is convenient to define the states associated with $\psi_{\boldsymbol{k},\uparrow(\downarrow)}$ pseudospin-up (down) particles. In this case, each pseudospin electron does not carry weight of more than one spin species of any orbital. Inversely, the decomposition of any

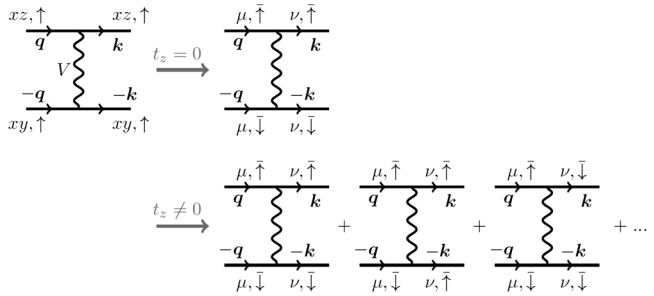

FIG. 1. Projection of a representative lowest order vertex into the pseudospin basis. The wavy lines denote the bare or projected Coulomb interactions. The diagram on the left originates from the bare Coulomb repulsion between the spin-up xz and xy electrons. The first and second line on the right-hand side are for spin-orbit entangled three-orbital models without and with direct interorbital xy-xz/yz hopping t_z, respectively. The summation over the band indices μ/ν are implicit. Note that only intraband pairing is considered. In addition, due to the peculiar form of the SOC, when $t_z = 0$ the spin-up (down) xy orbital is projected solely to the pseudospin-down (up) states in the band basis.

individual spin species of any orbital belongs with only one pseudospin species on the bands. Taking into account the on-site Coulomb interactions between the t_{2g} orbitals, a low-energy effective action in the Cooper channel can be constructed perturbatively by projecting the Coulomb interactions and the associated spin- or charge-fluctuation-mediated interactions onto the Fermi level [34,47,59].

A close inspection of the projection reveals that the bare Coulomb interactions do not lead to scatterings from equal-pseudospin Cooper pairs to opposite-pseudospin pairs, nor vice versa. More specifically, as explained in Ref. [82] and exemplified diagramatically in the first line of Fig 1, interactions such as the following are absent at this order:

$$\Gamma_{\boldsymbol{k},\boldsymbol{q}} a^{\dagger}_{\nu,\boldsymbol{k},\bar{\uparrow}} a^{\dagger}_{\nu,-\boldsymbol{k},\bar{\uparrow}} a_{\mu,-\boldsymbol{q},\bar{\uparrow}} a_{\mu,\boldsymbol{q},\bar{\downarrow}}, \tag{7}$$

where $\Gamma_{\boldsymbol{k},\boldsymbol{q}}$ denotes the projected effective interaction and $a^{\dagger}_{\mu,\bar{\sigma}}$ ($a_{\mu,\bar{\sigma}}$) creates (annihilates) a μ-band pseudospin-σ electron. Here the bar atop the spin symbol denotes the pseudospin basis. It can be further verified that effective interactions like Eq. (7) remain absent even when higher order scattering processes are considered. As a consequence, the x/y and z components of the $\vec{d}$ vector of the concerned pseudospin-triplet channel are decoupled. Hence, the $(k_x, k_y)\hat{z}$ and $(k_z\hat{x}, k_z\hat{y})$ pairings in general need not coexist, or shall condense at different temperatures if they do at low T.

However, in real material there always exists finite, albeit relatively weak, xy and xz/yz hybridization once interlayer coupling is considered. As is evident in Fig. 2 and as explained in more detail in Ref. [82], even a relatively weak interlayer hopping t_z between the xy and xz/yz orbitals could yield strong modifications to the details of the

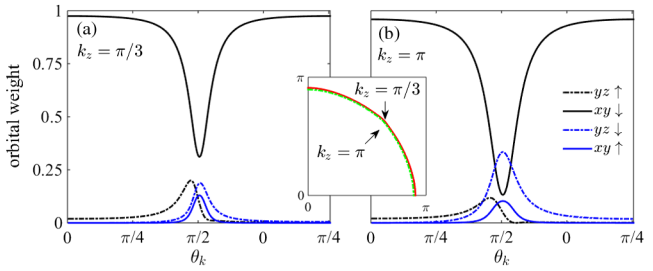

FIG. 2. Spin-resolved orbital weights across the γ-band Fermi surface at two different values of k_z in the three-band tight-binding model with $t_z = 0.05t$. The corresponding tight-binding model is given in Ref. [82]. Presented data are for the pseudospin-up states as defined in the text. Only the weights of the yz and xy orbitals are shown for clarity. In the horizontal axis θ_k stands for the angle of the Fermi momentum with respect to the x axis. Inset: Cross section of the γ-band Fermi surface at the two k_z's shown in (a) and (b).

electronic structure. The resultant pseudospins, especially those with momenta around the Brillouin zone diagonal, possess sizable weights of both spin species of all orbitals. Remarkably, this is achieved without introducing noticeable corrugation to the three-dimensional Fermi surface (inset of Fig. 2). We stress that the significant k_z dependence of the spin-orbit entanglement was also observed in spin-resolved photoemission studies [70]. The corresponding action now permits scattering processes like Eq. (7), as illustrated in the second line of Fig. 1 (see also Ref. [82]). In this case, the gap functions $(k_x, k_y)\hat{z}$ and $(k_z\hat{x}, k_z\hat{y})$ are inherently coupled and should emerge simultaneously at a single T_c.

Note that although the realistic pairing functions are likely more anisotropic than shown in Eq. (4), however, assuming the general relevance of the $(k_z\hat{x}, k_z\hat{y})$ pairing, here we are only interested in the nontrivial consequences of the resultant 3D odd-parity pairing.

Odd-parity nematic pairing.—We proceed to discuss the stable superconducting states associated with Eq. (4) in a single-band model for illustration. These $\vec{d}$ vectors lead to a simple expression for Eq. (3),

$$\beta' \approx C\langle k_x^2 k_y^2 - \epsilon^2 k_z^2 (k_x^2 + k_y^2 + \epsilon^2 k_z^2)\rangle_{\mathrm{FS}}. \tag{8}$$

Depending on the value of the anisotropic parameter ϵ, β' can take either signs. In Fig. 3, we sketched the sign of β' as

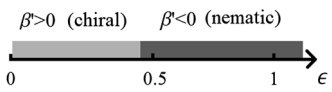

FIG. 3. The phase diagram as a function of ϵ. The chiral and nematic phases are shaded in light and dark gray, respectively. We assume cylindrical Fermi surface with radius 1 and replace k_z by $\sin k_z$ (taking the range of k_z to be $[-\pi, \pi]$ in the integral). In this calculation β' changes sign at $\epsilon_c \approx 0.46$.

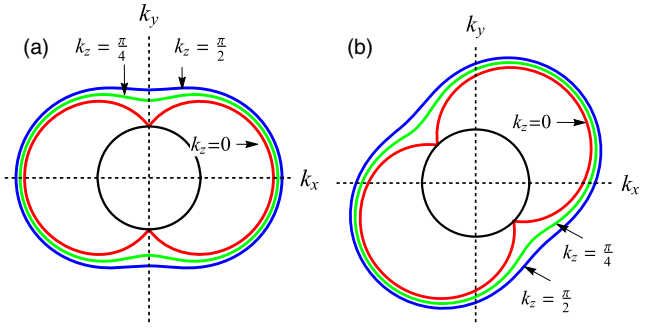

FIG. 4. Representative gap structure on the approximately cylindrical Fermi surface (black) for the (a) horizonal nematic and (b) diagonal nematic states with $\epsilon = 0.5$. As indicated, the three curves shown in each plot are for three values of k_z. In these calculations, we have replaced k_z in the gap function by $\sin k_z$.

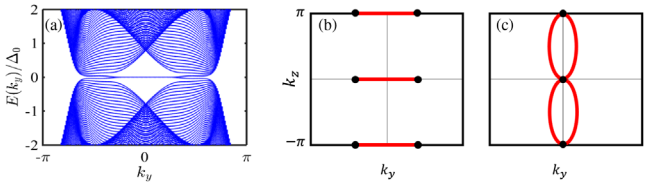

FIG. 5. (a) Low-energy spectra at fixed $k_z = 0$ for the diagonal nematic odd-parity pairing at $\epsilon = 0.8$ in a geometry with two (100) surfaces. In the lattice BdG calculations, the k_i's in the pairing functions are replaced by the simple lowest order harmonic $\sin k_i$. Note that the flat edge modes acquire some dispersion due to finite size effects. (b) Sketched arcs spanned by the surface zero modes in the nematic phase. (c) Sketched Majorana loops formed by the Majorana zero modes in the chiral phase.

a function of ϵ, assuming a cylindrical Fermi surface with radius $k_{F\|} = 1$ and taking $k_z \to \sin k_z$. Note that the critical value ϵ_c at which $\beta' = 0$ will in general be different in a more realistic model. As discussed, $\epsilon = \epsilon_c$ separates the TRSB and TRI phases. In the latter case, either a diagonal nematic state with $\boldsymbol{\phi} = \phi(1, \pm 1)$ or a horizontal one with $\boldsymbol{\phi} = \phi(1, 0)/(0, 1)$ could be more stable, depending on the details of the realistic band and gap structures [82].

For small $|\epsilon|$, $\beta' > 0$ and the system favors a TRSB chiral-like pairing ($\epsilon = 0$ returns the ordinary chiral p-wave) with a nodeless isotropic superconducting gap. This state is nonunitary, and it generates finite edge current. We do not further explore this possibility, but emphasize its intrinsic 3D nature if indeed realized in Sr_2RuO_4.

Below we focus on the TRI states, e.g., the horizontal nematic state $\boldsymbol{\phi} = \phi(1, 0)$. Its gap function $|\Delta_{\boldsymbol{k}}| = \Delta_0\sqrt{\epsilon^2 k_z^2 + k_x^2}$ reflects a breaking of the lattice C_4 symmetry down to C_2, with gap minima at $k_x = 0$ and maxima at $k_x = \pm k_F$ at each k_z. Hence it may be termed a "TRI nematic pairing." This state possesses nodal points at TRI k_z, i.e., $k_z = 0$ and $k_z = \pi$ upon replacing k_z by appropriate lattice harmonics in the gap function. Note that in other nematic states, the nodal-point directions are properly rotated. The representative gap structure at various k_z is shown in Fig. 4 for the two different types of nematic states.

One appealing feature of the nematic phase is the absence of spontaneous current at the edges due to TRI. In addition, at (100) or (010) surfaces, dispersionless edge modes with energy $\propto \epsilon k_z$ emerge for each k_z [Fig. 5(a)] for the case of diagonal nematic pairing. Note that the horizontal nematic state with $\boldsymbol{\phi} \sim (1, 0)$ supports surface states on the (100) surface, but not on the (010) surface. These surface states could be associated with the conductance peaks in the tunneling spectra [86,87]. Taking the (100) surface in the diagonal nematic state as an example, there should be two horizontal Majorana arcs within $k_y \in [-k_{F\|}, k_{F\|}]/\sqrt{2}$ at $k_z = 0$ and π [Fig. 5(b)]. By contrast, in the nonunitary chiral state, two singly-degenerate chiral edge modes appear [Fig. 5(c)] and finite edge current follows naturally. The zero modes in this case form two vertically connected and elongated Majorana loops, as depicted in Fig. 5(c). The peculiar surface spectra of the nematic and chiral states can be distinguished in photoemission and quasiparticle interference studies. Furthermore, the nematic states form the bases of a $U(1) \times Z_2$ field theory. The Z_2 symmetry permits the formation of domains characterized by the two degenerate pairing functions, much like what has been proposed for chiral p wave. This may be consistent with the signatures of domain formation observed in some experiments [11,88–91].

Discussions and summary.—Guided by symmetry considerations, we argued that the odd-parity E_u pairing in Sr_2RuO_4 acquires an inherent 3D form $(k_x\hat{z} + \epsilon k_z\hat{x}, k_y\hat{z} + \epsilon k_z\hat{y})$ in the presence of finite SOC and interorbital interlayer coupling. This leads to an appealing possibility of a novel TRI nematic odd-parity pairing, thereby providing an alternative perspective to understand the perplexing superconductivity in this material.

Besides resolving the notorious edge current problem, the nematic pairing may also explain some other outstanding puzzles. For example, compared with the chiral pairing, the nematic state could stand a better chance to explain the absence of split transitions under perturbations that break the degeneracy of the two E_u components [29–31]. With applied uniaxial strain along any generic direction, the splitting is expected for the scenario with the chiral ground state where a sequence of two transitions spontaneously break distinct symmetries: the $U(1)$ symmetry at the upper transition, and the time-reversal symmetry at the lower one. For the case of diagonal nematic pairing, a genuine second transition occurs only when a uniaxial strain is applied *exactly* parallel to the (100) or (010) direction. In this scenario, the lower transition breaks a reflection symmetry about the vertical plane parallel to the (100) or (010) direction. However, for any amount of misalignment in applied strain, as could be the case in a real experiment, no sharp lower transition should occur [92],

although a smeared crossover may appear to a degree that depends on the level of misalignment. Note also that, in the case of the horizontal nematic state, applying external strain along the (100) direction cannot give rise to split transitions.

Nevertheless, this nematic pairing needs to withstand the test of various other existing measurements, which remains to be carefully examined. Note that the absence of C_2 anisotropy in thermodynamic measurements under in-plane magnetic fields [93,94] could be consistent with nematic pairing because the externally applied field may drive a rotation of the nematic orientation. By contrast, in Bi_2Se_3 superconductors the nematic orientation may be pinned by a weak structural distortion as reported in Ref. [95]. The nematicity in Sr_2RuO_4 could be revealed in measurements like the angle-dependent in-plane Josephson tunneling [96] and the visualization of single vortex structure in scanning tunneling microscopy, as has been demonstrated for $Cu_xBi_2Se_3$ [97,98]. Regarding the contradiction between the point-nodal gap structure and the experimental indications of line-nodal pairing [24,25], we note that the realistic gap function could be more anisotropic. In particular, it is in principle possible to have, e.g., $\vec{d}_{1\boldsymbol{k}} = g_{\boldsymbol{k}}(k_x\hat{z} + \epsilon k_z\hat{x})$ and similarly for $\vec{d}_{2\boldsymbol{k}}$, where the form factor $g_{\boldsymbol{k}}$ carries horizontal or vertical line nodes. Such line nodes are not imposed by symmetry but could very likely arise in reality, given the highly anisotropic electronic structure in Sr_2RuO_4.

We are grateful to Fan Yang and Li-Da Zhang for stimulating discussions, and to Daniel Agterberg and Shingo Yonezawa for helpful communications. This work is supported in part by the MOST of China under Grants No. 2016YFA0301001 and No. 2018YFA0305604 and by the NSFC under Grant No. 11474175 (W. H. and H. Y.). W. H. also acknowledges the support by the C. N. Yang Junior Fellowship of the Institute for Advanced Study at Tsinghua University.

*yaohong@tsinghua.edu.cn

[1] Y. Maeno, H. Hashimoto, K. Yoshida, S. Nishizaki, T. Fujita, J. G. Bednorz, and F. Lichtenberg, Nature (London) **372**, 532 (1994).
[2] T. M. Rice and M. Sigrist, J. Phys. Condens. Matter **7**, L643 (1995).
[3] G. Baskaran, Physica (Amsterdam) **223B**, 490 (1996).
[4] K. Ishida, H. Mukuda, Y. Kitaoka, K. Asayama, Z. Q. Mao, Y. Mori, and Y. Maeno, Nature (London) **396**, 658 (1998).
[5] J. A. Duffy, S. M. Hayden, Y. Maeno, Z. Mao, J. Kulda, and G. J. McIntyre, Phys. Rev. Lett. **85**, 5412 (2000).
[6] K. D. Nelson, Z. Q. Mao, Y. Maeno, and Y. Liu, Science **306**, 1151 (2004).
[7] G. M. Luke *et al.*, Nature (London) **394**, 558 (1998).
[8] J. Xia, Y. Maeno, P. T. Beyersdorf, M. M. Fejer, and A. Kapitulnik, Phys. Rev. Lett. **97**, 167002 (2006).
[9] Y. Maeno, T. M. Rice, and M. Sigrist, Phys. Today **54**, 1, 42 (2001).
[10] A. P. Mackenzie and Y. Maeno, Rev. Mod. Phys. **75**, 657 (2003).
[11] C. Kallin and A. J. Berlinsky, J. Phys. Condens. Matter **21**, 164210 (2009).
[12] C. Kallin, Rep. Prog. Phys. **75**, 042501 (2012).
[13] Y. Maeno, S. Kittaka, T. Nomura, S. Yonezawa, and K. Ishida, J. Phys. Soc. Jpn. **81**, 011009 (2012).
[14] Y. Liu and Z. Q. Mao, Physica (Amsterdam) **514C**, 339 (2015).
[15] C. Kallin and A. J. Berlinsky, Rep. Prog. Phys. **79**, 054502 (2016).
[16] A. P. Mackenzie, T. Scaffidi, C. W. Hicks, and Y. Maeno, npj Quantum Materials **2**, 40 (2017).
[17] D. Vollhardt and P. Wölfle, *The Superfluid Phases of Helium 3* (Dover, New York, 1990).
[18] A. Y. Kitaev, Ann. Phys. (Amsterdam) **303**, 2 (2003).
[19] C. Nayak, S. H. Simon, A. Stern, M. Freedman, and S. Das Sarma, Rev. Mod. Phys. **80**, 1083 (2008).
[20] J. R. Kirtley, C. Kallin, C. W. Hicks, E.-A. Kim, Y. Liu, K. A. Moler, Y. Maeno, and K. D. Nelson, Phys. Rev. B **76**, 014526 (2007).
[21] C. W. Hicks, J. R. Kirtley, T. M. Lippman, N. C. Koshnick, M. E. Huber, Y. Maeno, W. M. Yuhasz, M. B. Maple, and K. A. Moler, Phys. Rev. B **81**, 214501 (2010).
[22] P. J. Curran, S. J. Bending, W. M. Desoky, A. S. Gibbs, S. L. Lee, and A. P. Mackenzie, Phys. Rev. B **89**, 144504 (2014).
[23] M. Matsumoto and M. Sigrist, J. Phys. Soc. Jpn. **68**, 994 (1999).
[24] S. Nishizaki, Y. Maeno, and Z. Q. Mao, J. Phys. Soc. Jpn. **69**, 572 (2000).
[25] E. Hassinger, P. Bourgeois-Hope, H. Taniguchi, S. RenedeCotret, G. Grissonnanche, M. S. Anwar, Y. Maeno, N. Doiron-Leyraud, and L. Taillefer, Phys. Rev. X **7**, 011032 (2017).
[26] K. Deguchi, M. A. Tanatar, Z. Q. Mao, T. Ishiguro, and Y. Maeno, J. Phys. Jpn. Soc. **71**, 2839 (2002).
[27] C. Rastovski, C. D. Dewhurst, W. J. Gannon, D. C. Peets, H. Takatsu, Y. Maeno, M. Ichioka, K. Machida, and M. R. Eskildsen, Phys. Rev. Lett. **111**, 087003 (2013).
[28] S. J. Kuhn, W. Morgenlander, and E. R. Louden, C. Rastovski, W. J. Gannon, H. Takatsu, D. C. Peets, Y. Maeno, C. D. Dewhurst, J. Gavilano, and M. R. Eskildsen, Phys. Rev. B **96**, 174507 (2017).
[29] S. Yonezawa, T. Kajikawa, and Y. Maeno, J. Phys. Soc. Jpn. **83**, 083706 (2014).
[30] C. W. Hicks, D. O. Brodsky, E. A. Yelland, A. S. Gibbs, J. A. N. Bruin, M. E. Barber, S. D. Edkins, K. Nishimura, S. Yonezawa, Y. Maeno, and A. P. Mackenzie, Science **344**, 283 (2014).
[31] A. Steppke, L. Zhao *et al.*, Science **355**, eaaf9398 (2017).
[32] P. E. C. Ashby and C. Kallin, Phys. Rev. B **79**, 224509 (2009).
[33] J. A. Sauls, Phys. Rev. B **84**, 214509 (2011).
[34] S. Raghu, A. Kapitulnik, and S. A. Kivelson, Phys. Rev. Lett. **105**, 136401 (2010).
[35] E. Taylor and C. Kallin, Phys. Rev. Lett. **108**, 157001 (2012).
[36] K. I. Wysokiński, J. F. Annett, and B. L. Györffy, Phys. Rev. Lett. **108**, 077004 (2012).

[37] Y. Imai, K. Wakabayashi, and M. Sigrist, Phys. Rev. B **85**, 174532 (2012); **88**, 144503 (2013).
[38] S. B. Chung, S. Raghu, A. Kapitulnik, and S. A. Kivelson, Phys. Rev. B **86**, 064525 (2012).
[39] S. Takamatsu and Y. Yanase, J. Phys. Soc. Jpn. **82**, 063706 (2013).
[40] T. L. Hughes, H. Yao, and X.-L. Qi, Phys. Rev. B **90**, 235123 (2014).
[41] J. W. Huo, T. M. Rice, and F. C. Zhang, Phys. Rev. Lett. **110**, 167003 (2013).
[42] Q. H. Wang, C. Platt, Y. Yang, C. Honerkamp, F. C. Zhang, W. Hanke, T. M. Rice, and R. Thomale, Europhys. Lett. **104**, 17013 (2013).
[43] A. Bouhon and M. Sigrist, Phys. Rev. B **90**, 220511(R) (2014).
[44] S. Lederer, W. Huang, E. Taylor, S. Raghu, and C. Kallin, Phys. Rev. B **90**, 134521 (2014).
[45] W. Huang, E. Taylor, and C. Kallin, Phys. Rev. B **90**, 224519 (2014).
[46] W. Huang, S. Lederer, E. Taylor, and C. Kallin, Phys. Rev. B **91**, 094507 (2015).
[47] T. Scaffidi, J. C. Romers, and S. H. Simon, Phys. Rev. B **89**, 220510(R) (2014).
[48] T. Scaffidi and S. H. Simon, Phys. Rev. Lett. **115**, 087003 (2015).
[49] K. Yada, A. A. Golubov, Y. Tanaka, and S. Kashiwaya, J. Phys. Soc. Jpn. **83**, 074706 (2014).
[50] M. Tsuchiizu, Y. Yamakawa, S. Onari, Y. Ohno, and H. Kontani, Phys. Rev. B **91**, 155103 (2015).
[51] N. Nakai and K. Machida, Phys. Rev. B **92**, 054505 (2015).
[52] Y. Amano, M. Ishihara, M. Ichioka, N. Nakai, and K. Machida, Phys. Rev. B **91**, 144513 (2015).
[53] J. A. Sauls, H. Wu, and S. B. Chung, Front. Phys. **3**, 36 (2015).
[54] S. Cobo, F. Ahn, I. Eremin, and A. Akbari, Phys. Rev. B **94**, 224507 (2016).
[55] Y.-T. Hsu, A. F. Rebola, C. J. Fennie, and E.-A. Kim, arXiv:1701.07884.
[56] B. Kim, S. Khmelevskyi, I. I. Mazin, D. F. Agterberg, and C. Franchini, npj Quantum Materials **2**, 37 (2017).
[57] L. Komendova and A. M. Black-Schaffer, Phys. Rev. Lett. **119**, 087001 (2017).
[58] J.-L. Zhang, W. Huang, M. Sigrist, and D.-X. Yao, Phys. Rev. B **96**, 224504 (2017).
[59] L.-D. Zhang, W. Huang, F. Yang, and H. Yao, Phys. Rev. B **97**, 060510(R) (2018).
[60] S. B. Etter, A. Bouhon, and M. Sigrist, Phys. Rev. B **97**, 064510 (2018).
[61] Y. Tada, W. Nie, and M. Oshikawa, Phys. Rev. Lett. **114**, 195301 (2015).
[62] M. H. Fischer and E. Berg, Phys. Rev. B **93**, 054501 (2016).
[63] A. Ramires and M. Sigrist, Phys. Rev. B **94**, 104501 (2016).
[64] W. Huang, T. Scaffidi, M. Sigrist, and C. Kallin, Phys. Rev. B **94**, 064508 (2016).
[65] T. Ojanen, Phys. Rev. B **93**, 174505 (2016).
[66] S.-I. Suzuki and Y. Asano, Phys. Rev. B **94**, 155302 (2016).
[67] Y. C. Liu, F. C. Zhang, T. M. Rice, and Q. H. Wang, npj Quantum Materials **2**, 12 (2017).
[68] Y.-T. Hsu, W. Cho, B. Burganov, C. Adamo, K. M. Shen, D. G. Schlom, C. J. Fennie, and E. A. Kim, Phys. Rev. B **94**, 045118 (2016).
[69] M. W. Haverkort, I. S. Elfimov, L. H. Tjeng, G. A. Sawatzky, and A. Damascelli, Phys. Rev. Lett. **101**, 026406 (2008).
[70] C. N. Veenstra, Z.-H. Zhu, M. Raichle, B. M. Ludbrook, A. Nicolaou, B. Slomski, G. Landolt, S. Kittaka, Y. Maeno, J. H. Dil, I. S. Elfimov, M. W. Haverkort, and A. Damascelli, Phys. Rev. Lett. **112**, 127002 (2014).
[71] C. G. Fatuzzo *et al.*, Phys. Rev. B **91**, 155104 (2015).
[72] L. Fu and E. Berg, Phys. Rev. Lett. **105**, 097001 (2010).
[73] L. Fu, Phys. Rev. B **90**, 100509(R) (2014).
[74] J. W. F. Venderbos, V. Kozii, and L. Fu, Phys. Rev. B **94**, 180504(R) (2016).
[75] K. Matano, M. Kriener, K. Segawa, Y. Ando, and G-Q. Zheng, Nat. Phys. **12**, 852 (2016).
[76] S. Yonezawa, K. Tajiri, S. Nakata, Y. Nagai, Z. Wang, K. Segawa, Y. Ando, and Y. Maeno, Nat. Phys. **13**, 123 (2017).
[77] Y. Pan, A. M Nikitin, G. K. Araizi, Y. K. Huang, Y. Matsushita, T. Naka, and A. de Visser, Sci. Rep. **6**, 28632 (2016).
[78] G. Du, Y. Li, J. Schneeloch, R. D. Zhong, G. Gu, H. Yang, and H.-H. Wen, Sci. China Phys. Mech. Astron. **60**, 037411 (2017).
[79] J. Shen, W-Y. He, Z. Huang, C-w. Cho, S. H. Lee, Y. S. Hor, K. T. Law, and R. Lortz, npj Quantum Materials **2**, 59 (2017).
[80] G. E. Volovik and L. P. Gor'kov, JETP Lett. **61**, 843 (1985).
[81] M. Sigrist and K. Ueda, Rev. Mod. Phys. **63**, 239 (1991).
[82] See Supplemental Material at http://link.aps.org/supplemental/10.1103/PhysRevLett.121.157002 for more detailed analyses of the role of SOC and interlayer inter-orbital hybridization, and a derivation of the Ginzburg-Landau free energy.
[83] M. E. Zhitomirsky and T. M. Rice, Phys. Rev. Lett. **87**, 057001 (2001).
[84] Y. Hasegawa, K. Machida, and M. Ozaki, J. Phys. Soc. Jpn. **69**, 336 (2000).
[85] J. F. Annett, G. Litak, B. L. Györffy, and K. I. Wysokinski, Phys. Rev. B **66**, 134514 (2002).
[86] S. Kashiwaya, H. Kashiwaya, H. Kambara, T. Furuta, H. Yaguchi, Y. Tanaka, and Y. Maeno, Phys. Rev. Lett. **107**, 077003 (2011).
[87] Y. A. Ying, Ph.D. thesis, The Pennsylvania State University, 2012, Chap. 6.
[88] F. Kidwingira, J. D. Strand, D. J. Van Harlingen, and Y. Maeno, Science **314**, 1267 (2006).
[89] K. Saitoh, S. Kashiwaya, H. Kashiwaya, Y. Mawatari, Y. Asano, Y. Tanaka, and Y. Maeno, Phys. Rev. B **92**, 100504 (R) (2015).
[90] H. Wang, J. Luo, W. Lou, J. E. Ortmann, Z. Q. Mao, Y. Liu, and J. Wei, New J. Phys. **19**, 053001 (2017).
[91] M. S. Anwar, R. Ishiguro, T. Nakamura, M. Yakabe, S. Yonezawa, H. Takayanagi, and Y. Maeno, Phys. Rev. B **95**, 224509 (2017).
[92] This is similar to the scenario in the classical Ising model, where the transition is smeared by any magnetic field except those applied precisely perpendicular to the Ising spins.
[93] Z. Q. Mao, Y. Maeno, S. NishiZaki, T. Akima, and T. Ishiguro, Phys. Rev. Lett. **84**, 991 (2000).
[94] K. Deguchi, Z. Q. Mao, H. Yaguchi, and Y. Maeno, Phys. Rev. Lett. **92**, 047002 (2004).

[95] A. Yu. Kuntsevich, M. A. Bryzgalov, V. A. Prudkogliad, V. P. Martovitskii, Yu. G. Selivanov, and E. G. Chizhevskii, arXiv:1801.09287.

[96] J. D. Strand, D. J. Bahr, D. J. Van Harlingen, J. P. Davis, W. J. Gannon, and W. P. Halperin, Science **328**, 1368 (2010).

[97] R. Tao, Y.-J. Yan, X. Liu, Z.-W. Wang, Y. Ando, T. Zhang, and D.-L. Feng, arXiv:1804.09122.

[98] The scanning SQUID can also image the vortex structure [21]. However, unlike STM, the current scanning SQUID measurements may not have the precision to resolve the nematic vortex shape.